Journal of Geoscience and Environment Protection, 2022, 10, 167-180
https://www.scirp.org/journal/gep
ISSN Online: 2327-4344
ISSN Print: 2327-4336

Preparation of Fe-Mg MOFs and Its Application in Removal of RhB and MO

Onyeka Samuel Ojinna[1], Yueli Wen[1*], Bin Wang[2], Chengda Li[2], Wei Huang[2,3], Ikeh Justin Tobechukwu[4]

[1]College of Environmental Science and Engineering, Taiyuan University of Technology, Taiyuan, China
[2]State Key Laboratory of Clean and Efficient Coal Utilization, Taiyuan University of Technology, Taiyuan, China
[3]Coal Conversion Technology & Engineering Co., Ltd., Taiyuan University of Technology, Taiyuan, China
[4]Geological Resources and Geological Engineering, Taiyuan University of Technology, Taiyuan, China
Email: *wenyueli@tyut.edu.cn

How to cite this paper: Ojinna, O. S., Wen, Y. L., Wang, B., Li, C. D., Huang, W., & Tobechukwu, I. J. (2022). Preparation of Fe-Mg MOFs and Its Application in Removal of RhB and MO. *Journal of Geoscience and Environment Protection, 10,* 167-180.
https://doi.org/10.4236/gep.2022.104011

Received: February 28, 2022
Accepted: April 21, 2022
Published: April 24, 2022

Abstract

The world wide application of dyes in papermaking, fabric, lithography, leather and other industrial production, has attracted more attention, due to water pollution caused by these organic dyes. Metal-organic frameworks (MOFs) which are a physical adsorption method of wastewater treatment are a kind of special three-dimensional crystal-like constituents built by multipurpose ligands and metallic ion classes, showing an advantage in removal of pollutants from solutions because of its unique properties are convenient for operation, high removal efficiency, and low cost. In this study, we investigated Fe-Mg based metal organic framework, Fe-Mg MOFs which was directly synthesized by the hydrothermal method. The obtained materials were analyzed with XRD, FT-IR, TG-DTG, SEM etc. and used for the treatment of printing and dyeing wastewater. The results showed that it has good adsorption performance for cation dye rhodamine B (RhB) and anion dye methyl orange (MO) in a wide pH range. The Fe-Mg MOF even after the 4th run, the Fe-Mg MOF catalyst still maintained nearly the initial catalytic activities. The kinetic studies revealed the adsorption process of the both contaminants obeys a pseudo-second order model. In addition, the equilibrium adsorption data of RhB and MO are in good agreement with Langmuir models. The maximum adsorption capacities are 694.44 and 236.97 mg/g at 308 K respectively. This work synthesizes a promising dual-functional adsorbent that can remove cationic and anionic dyes, which provide potential applications for actual wastewater treatment.

Keywords

Metal-Organic Frameworks (MOFs), Adsorption, Cationic and Anionic Dyes, Wastewater Treatment

1. Introduction

The water pollution caused by organic dyes has attracted more attention, because dyes are widely applied in papermaking, fabric, lithography, leather and other industrial production (de Sá, Cunha, & Nunes, 2013). The water is toxic with complex composite, deep color, and concentrated refractory organic matters. And it will bring about a threat to agriculture and food chain, and consequently to human health which are carcinogenic, teratogenic, and genetic mutation (Shan et al., 2015). Wastewater treatment has become a major problem in global water treatment.

In recent years, researchers have adopted biodegradation (Shi et al., 2021; Srinivasan & Sadasivam, 2021), chemical oxidation (Liu, Ohko, Zhang, Yang, & Zhang, 2010), membrane treatment technology (Jin et al., 2021), coagulation (Hussein & Jasim, 2021; Mcyotto et al., 2021), photocatalysis (Le, Akhtar, Park, Lee, & Yang, 2012; Mahlambi et al., 2013) and other technologies in the treatment of printing and dyeing wastewater. By comparison, it has been found that the physical adsorption method has the following merits, like convenient operation, high removal efficiency, and low cost. Metal-organic frameworks (MOFs) which are a physical adsorption method of wastewater treatment are a kind of special three-dimensional crystal-like constituents built by multipurpose ligands and metallic ion classes, showing an advantage in removal of pollutants from solutions (Zhang et al., 2020). Single metal MOFs, like Ni-MOFs (Zhao et al., 2017), Zn-MOFs (Yang et al., 2018), Cu-MOFs (Hu et al., 2014), Fe-MOFs (Wei, Chen, Liang, & Zhao, 2018), Zr-MOFs (Chen, Feng, & Wei, 2019), Al-MOFs (Tehrani & Zare-Dorabei, 2016) as well as double metal MOFs, like Zn-Co MOFs (Noor, Raffi, Iqbal, Yaqoob, & Zaman, 2019), Ni-Cu MOFs (Hu et al., 2014) etc., have been extensively applied in elimination of dyes from wastewater. MOFs have received great attention owing to their great excellent properties, such as versatile porous structures and numerous potential applications. In general, the elastic and extremely porous structures of MOFs facilitate the diffusion of guest ions or molecules easily into the bulk structure. Also, both the size and shape of the formed pores help in increasing the selectivity of adsorbing definite ions or molecules. These distinct advantages make MOFs ideal sorbents in dye absorption. MOFs have been recognized as promising adsorbents for bulky dyes removal from wastewater due to their tunable organic functionalities and diverse metal compositions. MOFs have an important advantage in that various frameworks can be formed by the participation of several metal cations. MOFs can be synthesized with specific properties to improve their performances in reaching the desired targets by deliberately and systematically setting their functionalities and structures; for example, the surface area, pore size and/or shape can be controlled by varying the connectivity of the cations and the type of the organic ligands. MOFs have been used in different potential applications as drug delivery, catalytic reactions, sensing and gas adsorption/separation. In this paper, Fe-Mg MOFs was synthesized and used to remove organic pollutants rhodamine B

(RhB) and methyl orange (MO) from wastewater after calcination and it showed an excellent performance. Furthermore, the effects of numerous elements such as adsorbent dosage, initial concentrations, solution pH, and contact time were evaluated. The adsorption kinetics and adsorption isotherms were also analyzed using theoretical models. In addition, the reusability of the adsorbent was tested.

2. Experimental

2.1. Materials

$Mg(NO_3)_2{\cdot}6H_2O$, $Fe(NO_3)_3{\cdot}9H_2O$, terephthalic acid and dimethylformamide (DMF) are purchased from Sigma Aldrich.

2.2. Apparatus

X-ray diffraction analysis (XRD) was performed on a DX-2700 X-ray diffractometer (Rigaku Corporation), with the Cu Kα radiation (λ = 0.15418 nm). N_2 adsorption-desorption isotherms (BET) were measured on a QDS-30 physical adsorption instrument (Kanta, USA) at liquid nitrogen temperature (77 K). The specific surface area was calculated by BET (Brunauer-Emmett-Teller) method, and the pore volume and pore diameter were calculated by the BJH (Barret-Joyner-Halenda) method. Scanning electron microscopy (SEM) was performed on a Quanta 400 FEG field emission electron microscope with an accelerating voltage of 20 kV, and EDS-mapping was applied in analyzing the element distribution on the catalyst surface.

2.3. Preparation of the Absorbent

Fe-Mg bimetallic Organic Frameworks were synthesized according to the literature (Noor et al., 2019), 1 mmol $Mg(NO_3)_2{\cdot}6H_2O$, 1 mmol $Fe(NO_3)_3{\cdot}9H_2O$ and 1 mmol terephthalic acid (H_2BDC) were dissolved in 10 mL DMF solution at a continuous shaking. The mix was moved to a Teflon-lined autoclave and blended homogeneously and heated at 120˚C for 8 hours. Afterwards, cooling to a room temperature was done, the solid was recovered by centrifugation, cleaned with DMF for many times, and desiccated at 120˚C. The obtained solid was named as Fe-Mg MOFs.

2.4. Adsorption Experiments

In a typical run, certain quantity of Fe-Mg MOFs (50, 100, 150, 200 mg) was added into 50 mL of RhB/MO dye solution of different concentration and stirred for a certain time at room temperature (30, 60, 90, 120, 150 minutes…). Then, the suspensions were separated by centrifugation for analysis. The solution was tested by UV-vis spectrophotometer at 552 nm (RhB) and 464 nm (MO), respectively. The removal efficiency and adsorption capacity at equilibrium were computed with the formulas (1) and (2):

$$\text{Removal efficiency}(\%) = \frac{C_0 - C_t}{C_0} * 100\% \quad (1)$$

$$q_e = \frac{(C_0 - C_e)V}{m} \quad (2)$$

with C_0 and C_e (mg/L) being the initial and equilibrium concentration of RhB/MO mixture respectively, q_e being the equilibrium adsorption capacity (mg/g), m (g) being the mass of the added adsorbents, and V (L) is the volume of the RhB/MO mixture.

3. Results and Discussion

3.1. Characterization

3.1.1. SEM

Figure 1 shows the SEM and outlook of the sample. From the inlet picture, it can be seen that the sample was brown powder. As shown in SEM diagram, the powder is composed by quadrangular with the width and length of 0.35 μm and 2.90 μm, respectively. It is interesting that the two sides of the quadrangular are truncated and become rectangular pyramid.

3.1.2. XRD and BET Analysis

The Brunauer-Emmett-Teller (BET) method is commonly applied to calculate the specific surface area on the basis of nitrogen desorption isotherm measurements at 77 k (8 - 10). Usually, data in the relative pressure range from 0.05 to 0.3 are used. As shown in Figure 2(a), compared with the simulated XRD as mentioned in literature (Noor et al., 2019), Fe-Mg MOFs was successfully prepared. Figures 2(b)-(d) show the N_2-adsorption-desorption isotherms, pore size distribution curve and Horvath-Kawazoe Differential Pore Volume Plot of the Fe-Mg MOFs, which indicate the catalyst is composed of mesoporous and macroporous structure. In a typical BET analysis, NM surface is determined from the volume of N_2 gas adsorbed on the NMs. N_2 gas is assumed to have access to the entire NM surface. The surface area measurements are based on adsorption of gas molecules in infinite layers with no interlayer interaction. Under these conditions, the basic Langmuir theory can be applied to each layer to derive the BET surface area for NMs (S_{BET}).

$$S_{BET} = V_0 N_a s / M_v \quad (3)$$

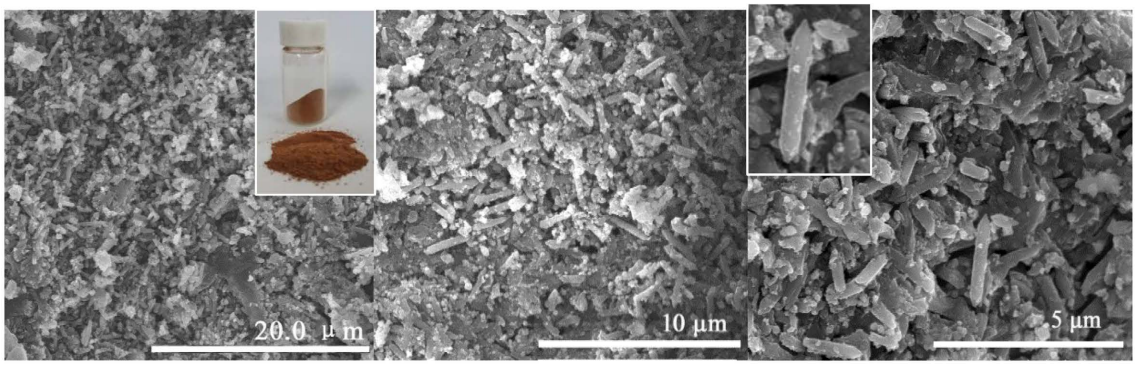

Figure 1. Outlook and SEM of Fe-Mg MOFs.

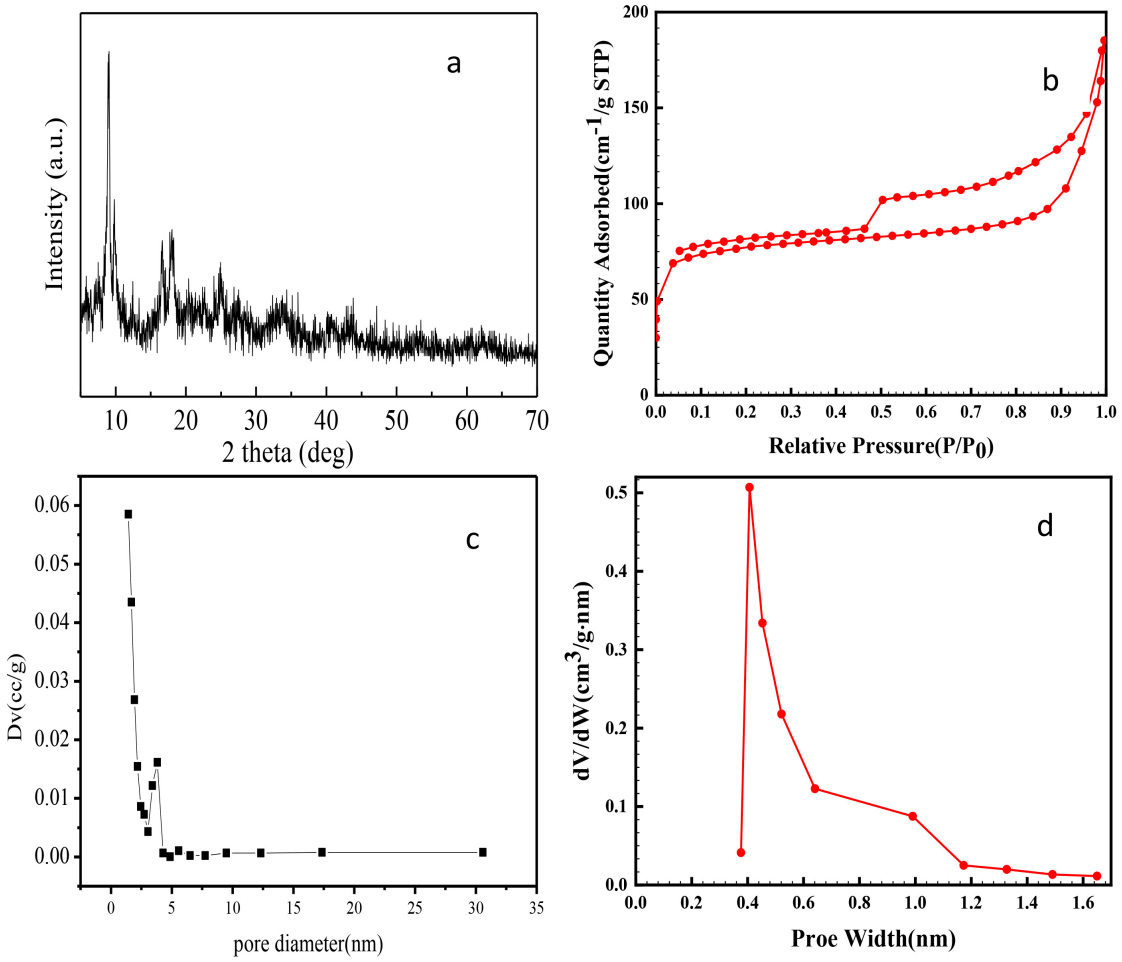

Figure 2. XRD pattern (a), N_2-adsorption-desorption isotherms (b), pore size distribution curve (c) and Horvath-Kawazoe Differential Pore Volume Plot (d) of the Fe-Mg MOFs.

where, V_0 is the volume of single monolayer of absorbed gas, N_a is Avogadro's number, M_v is molar volume of gas adsorbate and s is the surface area of a single gas molecule adsorbed on the solid. **Table 1** lists the texture parameters of the Fe-Mg MOFs adsorbent. The figure shows that the specific surface area is 379.18 m^2/g, which was examined by N_2 adsorption/desorption analysis at −196˚C, the HK Median pore width is about 0.58 nm, which further confirms that the Fe-Mg MOFs has both mesopores and micropores.

3.1.3. TG and DTG Analysis

As shown in **Figure 3**, the MOFs material has poor thermal stability. The weight loss of 3.45% appearing at 26˚C - 118˚C is assigned to desorption of the adsorptive water on the surface and MOFs inner structures. 7.18% of weight loss at 118˚C - 236˚C is attributed to desorption of solvent DMF. From 236˚C the ligand of terephthalic acid in the MOFs structure begins to decompose to carbon species, it reaches a weigh loss of 14.11% until to 350˚C. The last weight loss of 42.82% takes place in 350˚C - 440˚C, which can be specified to the combustion of carbon.

Table 1. Texture parameters of the Fe-Mg MOFs.

Adsorbent	Surface Area (m^2/g)	Pore Volume (cm^3/g)	HK Median Pore width (nm)	Average Pore Diameter (nm)
Fe-Mg MOFs	379.18	0.14	0.58	2.11

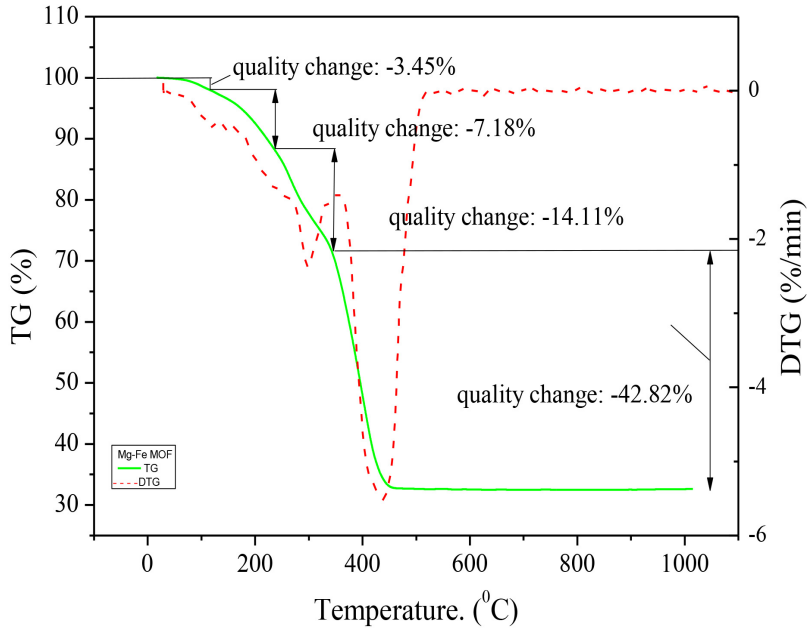

Figure 3. TG and DTG curves of Mg-Fe MOFs adsorbent.

3.1.4. FT-IR Analysis

The FTIR spectrum of **Figure 4** shows a primary specific top at about 3397 cm^{-1} attributed to the H-O-H stretching vibrations. The points that are observed at 1579 cm^{-1} for Fe-Mg MOFs could be allotted for the strong stretching shaking of C=O arising from -COOH, which can be recognized as the content of terephthalic acid in the MOF (Gu et al., 2019). The point at about 1386 cm^{-1} is because of the C-O stretching vibration. The three points at 1016, 1097 and 1153 cm^{-1} are specified for the twisting shaking of the hydroxyl group from M-OH (Zhang, Yao, Xiang, & Chen, 2014) and the replacement of the aromatic ring is appeared at 825 cm^{-1}. These outcomes propose that the structure of Fe-Mg-MOF comprises of the elementary terephthalic acid skeleton and the carboxyl groups of terephthalic acid are deprotonated. Furthermore, the points at 759, 823 and 887 cm^{-1} were attributed to metal-oxygen vibrations (Li, Deng, Yu, Huang, & Lim, 2010).

3.1.5. EDX Analysis from SEM

The EDX analysis of SEM (**Figure 5**) shows that Fe, Mg, C and O elements were detected in the absorbent, confirming that terephthalic acid existing in the MOFs structure. According to the relative molar ratio of the elements, the ratio Mg: Fe is about 0.1:1, which could be further adjusted to enhance the stability of the MOFs structure.

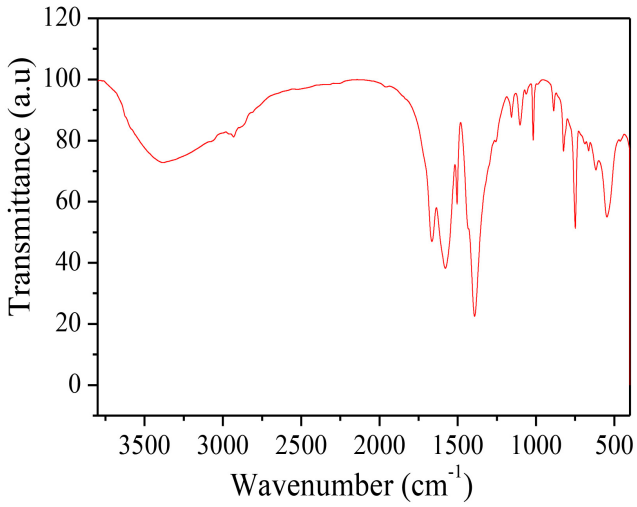

Figure 4. FT-IR spectrum of Mg-Fe MOFs adsorbent.

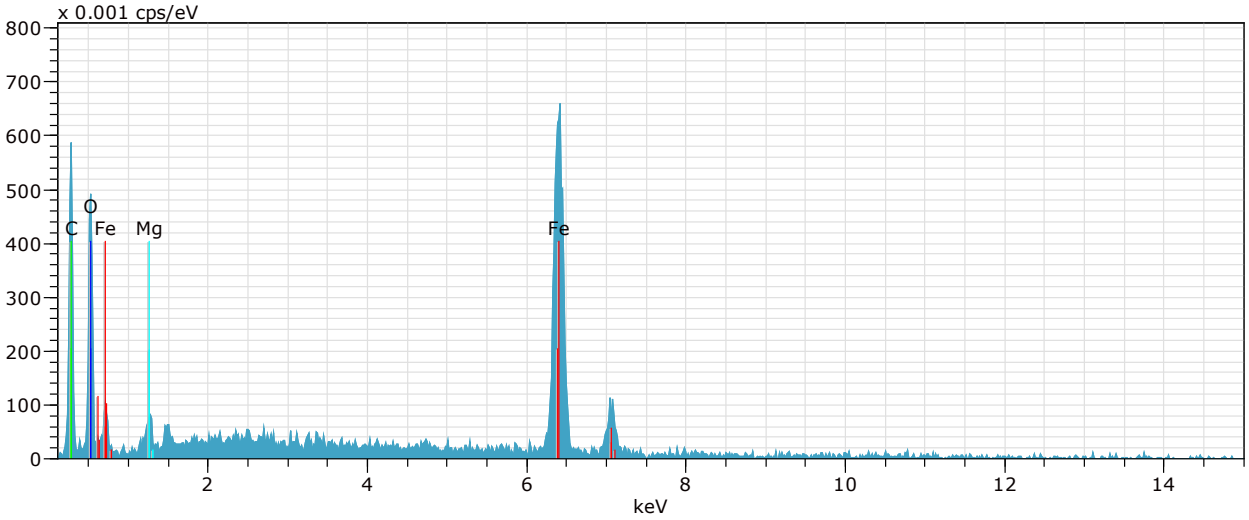

Figure 5. EDX analysis from SEM.

3.2. Adsorptive Property

3.2.1. Effects of Adsorbent Dosage and Initial Concentration

The adsorbent dosage has some influence in the removal efficiency of the dyes. The experiments of water regeneration were done in a 50 mL of 50 mg/L dye solution with diverse amount of absorbent Mg-Fe MOFs (50 mg, 100 mg, and 150 mg). As shown in **Figure 6(a)**, the results show that as the dosage of Mg-Fe MOFs (50 mg - 150 mg) increases, the removal efficiency of RhB and MO is almost stable, maintaining higher than 99.85%. The increase in removal efficiency is related to the sufficient adsorption sites of Mg-Fe MOFs. That might because that the initial concentration is not very high that the minimum dosage (50 mg) is enough for the dye. The changes caused by the initial concentration of RhB and MO solution (10 to 125 mg/L) on the removal efficiency was studied with 100 mg Mg-Fe MOFs as adsorbent (shown in **Figure 6(b)**). The removal efficiencies of RhB and MO dyes both increase firstly with the rise of the initial

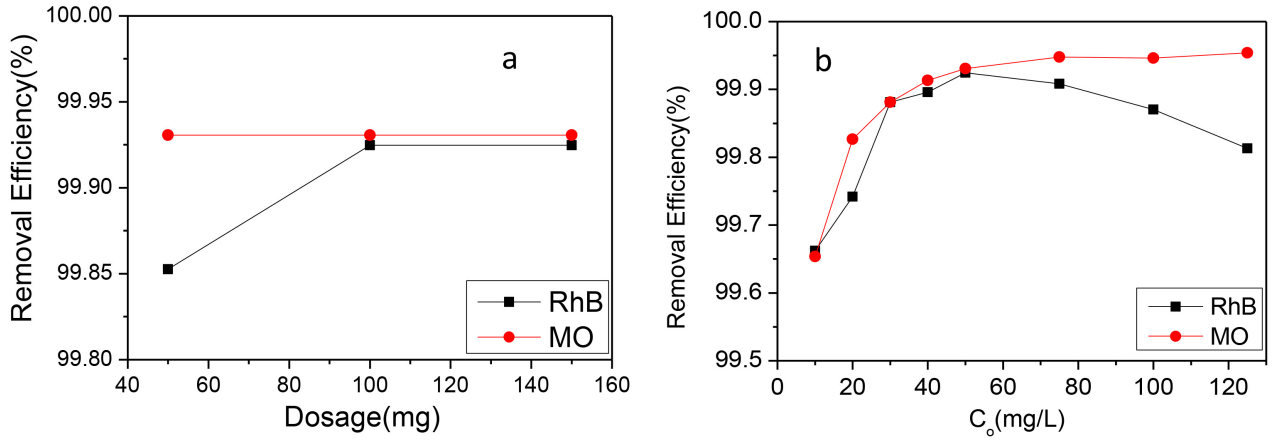

Figure 6. The effect of absorbent dosage and initial concentation on removal efficiency of RhB and MO.

concentration from 10 to 50 mg/L, but it shows much difference from the initial concentration of 75 mg/L. The removal efficiency for MO slightly goes up with the initial concentration increasing, while that for RhB dyes begin to decline when RhB initial concentration surpasses 50 mg/L, which suggests that it becomes more than its adsorption saturation value and cannot adsorb anymore. Otherwise the removal efficiency for RhB is still above 99.6%. The results also manifest that this absorbent shows good performance for both of MO and RhB, but even better for removal MO than RhB.

3.2.2. Effects of Contact Time and PH

As seen in **Figure 7(a)** and **Figure 7(b)**, the figures show the consequence of contact time on the removal efficiency for MO (a) and RhB (b) with the initial concentrations of 125 mg/L, different amount of Mg-Fe MOFs were considered (50 mg, 100 mg, 150 mg). It is found that the equilibrium can be reached at about 50 minute. It suggests that Mg-Fe MOFs can absorb the dyes very quickly.

pH is one of the important factors affecting adsorption efficiency. In the adsorption experiments, the pH value was regulated with 0.10 mol/L HCL or NaOH solution. The test was conducted with pH of 1, 3, 5, 7, 9, 11 and 13. From **Figure 7(c)** it can be observed that pH has less influence on the removal efficiency, which is relatively stable, and has no major change within the pH test scope for both RhB and MO. Through research, it is proved that Mg-Fe MOFs does not need to adjust the pH value when removing RhB or MO, which can simplify the operation steps and be economical for application. It proves that Mg-Fe MOFs is expected to be a simple and economical adsorbent for removing RhB and MO.

3.2.3. Effect of Contact Time on Adsorption Kinetics

The adsorption kinetics of Mg-Fe MOFs for RhB and MO were studied by pseudo-first order kinetic model (Equation (3)), pseudo-second order kinetic model (Equation (4)), intra-particle diffusion model (Equation (5)).

$$\log\left(q_e - q_t\right) = \log q_e - \frac{k_1 t}{2.303} \tag{4}$$

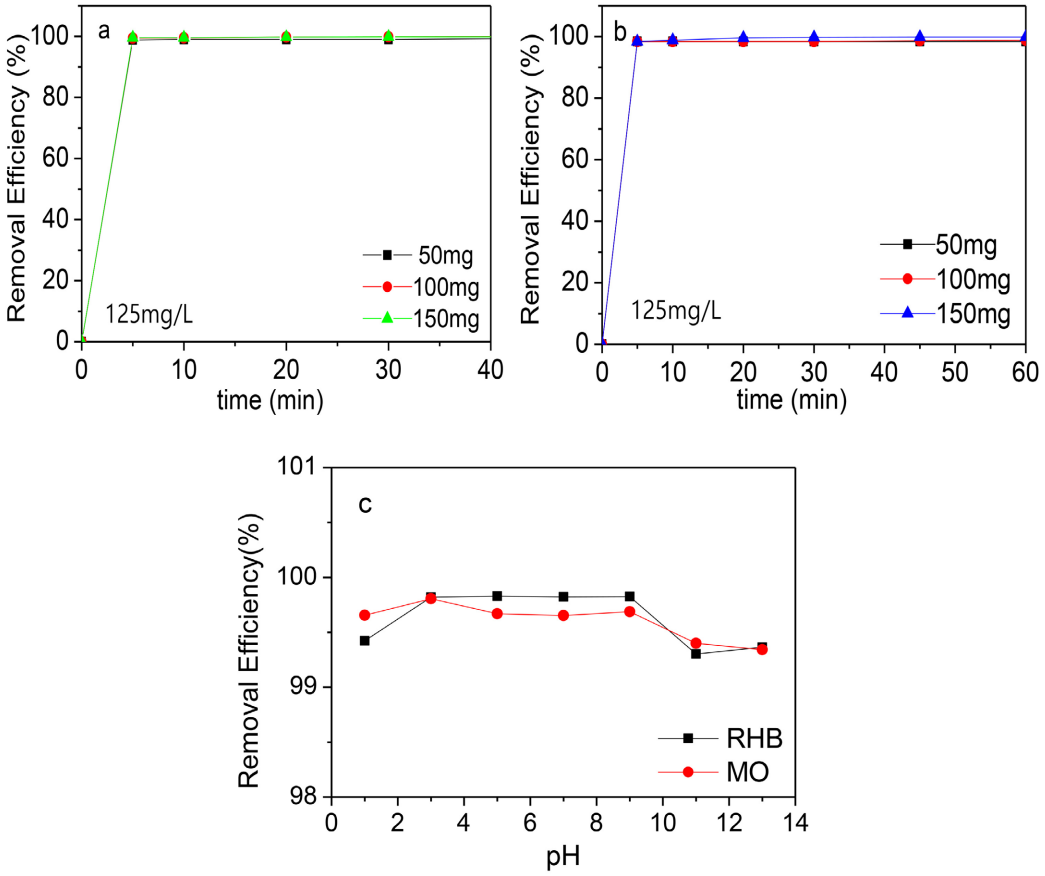

Figure 7. The effect of contact time (a for MO, b for RhB) and pH (c) on removal efficiency of MO and RhB dye with the initial concentration of 125 mg/L.

$$\frac{t}{q_t} = \frac{1}{k_2 q_e^2} + \frac{t}{q_e} \tag{5}$$

$$q_t = k_i t^{0.5} + C_i \tag{6}$$

where k_1 (min^{-1}), k_2 ($g \cdot mg^{-1} \cdot min^{-1}$), k_i ($mg \cdot g^{-1} \cdot min^{-1/2}$) are the pseudo-first order, pseudo-second order and intraparticle diffusion model rate constant, q_e and q_t ($g \cdot mg^{-1}$) are the adsorption capacity of the adsorbent for a certain dye molecular at equilibrium and at time t (min), respectively. The values of k_1 and q_e are calculated from the slope and intercept of plots of $\log(q_e - q_t)$ versus t. The values of k_2 and q_e can be obtained by plots of t/q_t versus t (**Figure 8(a)**, **Figure 8(b)**). k_i and C_i are the intra-particle diffusion rate constant and intercept of stage i, respectively. The values of the kinetic parameters and correlation coefficients (R^2) of the kinetic model are given in **Table 2**. The value of the correlation coefficient R^2 of the pseudo-second order model was very close to 1, and the values of q_e and $q_{e,cal}$ of theoretical adsorption capacity were basically consistent with the experimental adsorption capacity. This result shows that the adsorption process of RhB and MO follows the pseudo-second order model. Otherwise the adsorption capacity of MO was much higher than that of RhB. This indicates that the removal mechanism of RhB is the same with that for MO.

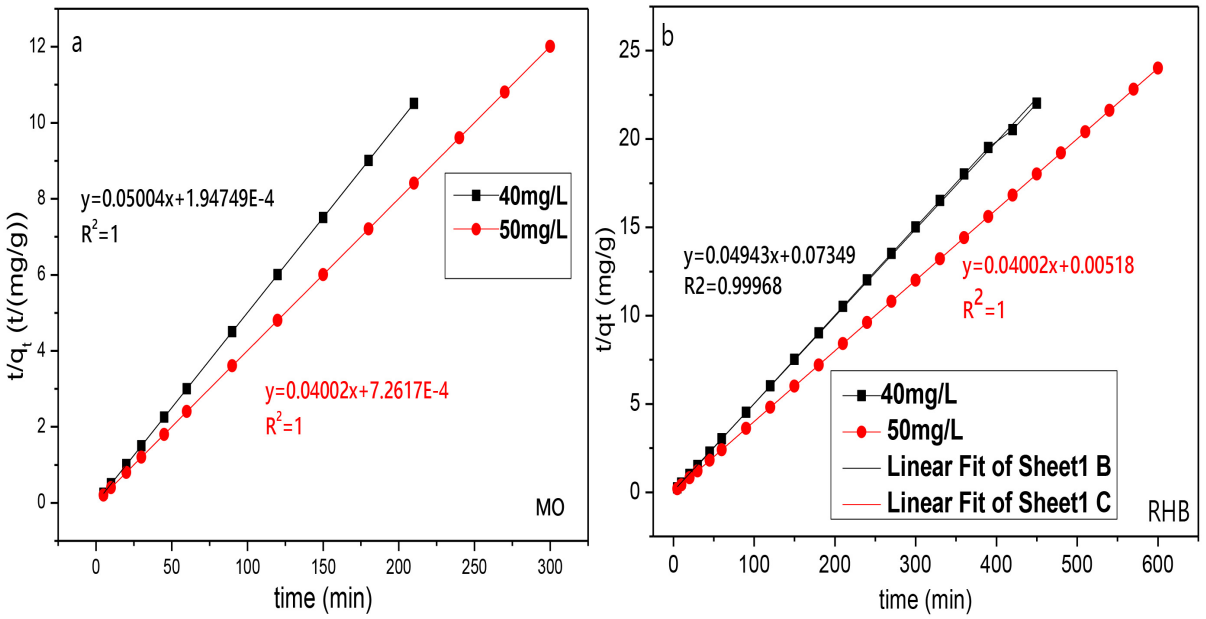

Figure 8. Pseudo-Second order kinetic plots adsorption of MO (a), and RhB (b), on Mg-Fe MOF.

Table 2. Comparison of pseudo-first order, pseudo-second order adsorption constants for dyes adsorption on Mg-Fe MOF.

Adsorbate	C_0	q_e	Pseudo-first order model			Pseudo-second order model		
			$q_{e,cal}$	$k_1 \times 10^{-6}$	R^2	$q_{e,cal}$	$k_2 \times 10^{-2}$	R^2
RhB	40	19.983	1.149	−1.22	0.5950	20.23	3.32	0.9997
	50	24.981	1.209	−2.72	0.3530	24.99	30.91	1.0000
MO	40	19.983	1.010	−1.08	0.3250	19.98	0.13	1.0000
	50	24.983	1.020	−3.62	0.5950	24.99	0.02	1.0000

3.2.4. Adsorption Isotherms

Adsorption isotherm studies related to adsorbent capacity and solute surface interaction. The Langmuir isotherm model that assumes monolayer sorption and Freundlich isotherm model that assumes a heterogeneous sorption are generally used isotherms to explain the solid-liquid adsorption system. The Langmuir (see Equation 7) and Freundlich (see Equation 8) isotherm models are applied in analyzing the experimental equilibrium adsorption results. The equations are as follows:

$$q_e = \frac{q_m K_L C_e}{1 + K_L C_e} \tag{7}$$

$$q_e = K_F C_e^{\frac{1}{n}} \tag{8}$$

where C_e (mg·L^{-1}) is the equilibrium concentration of the dye in solution, q_e (mg·g^{-1}) and q_m (mg·g^{-1}) are the equilibrium and theoretical maximum adsorption capacity, K_L and K_F are the Langmuir and Freundlich constants, n is the adsorption strength. If $2 < n < 10$, the adsorption process is difficult to proceed. If

$n < 2$, the adsorption is easy to proceed. The calculated parameters are listed in Table 3.

The adsorption capacity for RhB increased with the temperature increasing (shown in Figure 9(a)), which indicates that the adsorption process for RhB with Mg-Fe MOF is endothermic. The average R^2 value of the Langmuir isotherm

Table 3. Parameters of Langmuir and Freundlich isotherms for dyes adsorption on Mg-Fe MOF.

Adsorbate	T(K)	Langmuir			Freundlich		
		q_m	K_L	R^2	K_F	n	R^2
RhB	298	185.53	0.025	0.9996	3.730	1.15	0.9964
	308	213.68	0.005	0.9998	3.540	1.05	0.9986
	318	694.44	0.015	0.9999	4.970	1.16	0.9967
MO	298	105.04	0.073	0.9987	3.940	1.15	0.9946
	308	183.49	0.027	1.0000	5.480	1.20	0.9953
	318	236.97	0.014	0.9998	8.340	1.42	0.9858

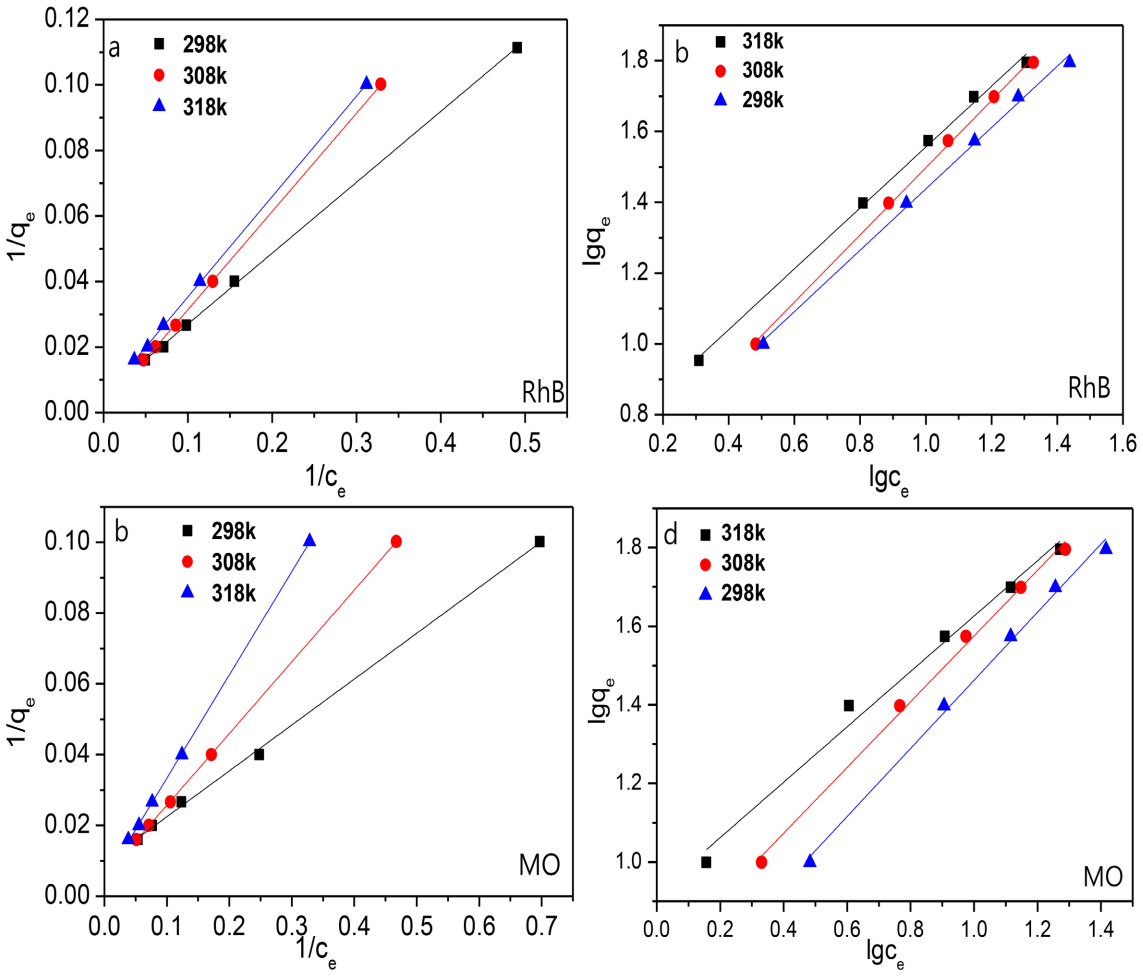

Figure 9. Fitting curve of Langmuir (a, c) and Freundlich (b, d) adsorption isotherms of RhB/MO on Mg-Fe MOF.

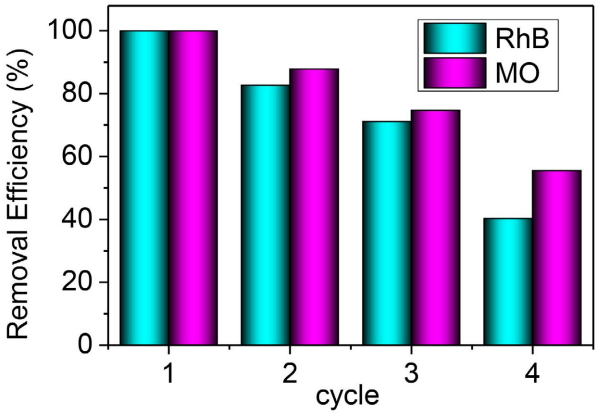

Figure 10. Reusability of Fe-Mg (0.1:1) MOFs for RhB and MO adsorption.

model is the closest to 1, indicating that Langmuir is most suitable for experimental data. According to the calculation, the fitted correlation coefficients was 0.9999 (318 K), which are larger than the fitting result of the Freundlich adsorption isotherm model (0.9986). The maximum adsorption capacity for RhB was 694.97 mg/g (318 K).

For MO, the Langmuir adsorption isotherm model was also better to describe the adsorption process with Mg-Fe MOF better than Freundlich adsorption isotherm model, and maximum adsorption capacity was 236.97 mg/g (318 K).

The experiment of regeneration and multiple cycles of Mg-Fe MOF are shown in **Figure 10**. The used Mg-Fe MOF was washed with ethanol after each use, which was followed by centrifugal separation and drying at 70˚C to obtain the regenerated adsorbent. After recovery, the adsorption experiment was repeated under the same conditions. The results showed that the adsorption of RhB/MO by Mg-Fe MOF can be used 4 times. The results showed that the adsorption of MO by Mg-Fe MOF still has a high adsorption capacity after four regenerations. After four cycles, the Removal efficiency for MO could maintain 99.716%. But after four regenerations, the adsorption capacity of Mg-Fe MOF for RhB was significantly reduced. After four cycles, the adsorption efficiency for RhB could maintain 99.46%.

4. Conclusion

Mg-Fe MOF was directly synthesized by the hydrothermal method, and the effects of adsorbent dosage, initial dye concentration, pH, and contact time on the adsorption of dye solution were systematically studied. It is found that the pH value has little effect on the adsorption. The adsorption of RhB and MO conforms to the pseudo-second-order kinetic model. The adsorption isotherm model of Fe-Mg MOF for RhB and MO removal obeyed Langmuir and Freundlich adsorption isotherm model, respectively. Fe-Mg MOF attracted RhB by an electrostatic force.

The large steric hindrance of RhB, did not prevent it from entering into the layers that were why the maximum adsorption capacity of Fe-Mg MOF for RhB

is far higher than that for MO despite MO having linear molecule which makes it easy to get into the layers or pores of Fe-Mg MOF. From the perspective of the adsorption performance of the adsorbent, Fe-Mg MOF with a layered structure that is easy to synthesize and is a promising and efficient adsorbent for removing anions dyes (RhB) and cationic (MO).

Conflicts of Interest

The authors declare no conflicts of interest regarding the publication of this paper.

References

Chen, D., Feng, P. F., & Wei, F. H. (2019). Preparation of Fe (III)-MOFs by Microwave-Assisted Ball for Efficiently Removing Organic Dyes in Aqueous Solutions under Natural Light. *Chemical Engineering Processing-Process Intensification, 135,* 63-67. https://doi.org/10.1016/j.cep.2018.11.013

de Sá, F. P., Cunha, B. N., & Nunes, L. M. (2013). Effect of pH on the Adsorption of Sunset Yellow FCF Food Dye into a Layered Double Hydroxide (CaAl-LDH-NO_3). *Chemical Engineering Journal, 215-216,* 122-127. https://doi.org/10.1016/j.cej.2012.11.024

Gu, Y., Xie, D., Wang, Y., Qin, W., Zhang, H., Wang, G. et al. (2019). Facile Fabrication of Composition-Tunable Fe/Mg Bimetal-Organic Frameworks for Exceptional Arsenate Removal. *Chemical Engineering Journal, 357,* 579-588. https://doi.org/10.1016/j.cej.2018.09.174

Hu, J., Yu, H., Dai, W., Yan, X., Hu, X., & Huang, H. (2014). Enhanced Adsorptive Removal of Hazardous Anionic Dye "Congo Red" by a Ni/Cu Mixed-Component Metal-Organic Porous Material. *RSC Advances, 4,* 35124-35130. https://doi.org/10.1039/C4RA05772D

Hussein, T. K., & Jasim, N. A. (2021). A Comparison Study between Chemical Coagulation and Electro-Coagulation Processes for the Treatment of Wastewater Containing Reactive Blue Dye. *Materials Today: Proceedings, 42,* 1946-1950. https://doi.org/10.1016/j.matpr.2020.12.240

Jin, P., Zhu, J., Yuan, S., Zhang, G., Volodine, A., Tian, M. et al. (2021). Erythritol-Based Polyester Loose Nanofiltration Membrane with Fast Water Transport for Efficient Dye/Salt Separation. *Chemical Engineering Journal, 406,* Article ID: 126796. https://doi.org/10.1016/j.cej.2020.126796

Le, T. T., Akhtar, M. S., Park, D. M., Lee, J. C., & Yang, O. B. (2012). Water Splitting on Rhodamine-B Dye Sensitized Co-Doped TiO_2 Catalyst under Visible Light. *Applied Catalysis B: Environmental, 111,* 397-401. https://doi.org/10.1016/j.apcatb.2011.10.023

Li, Z., Deng, S., Yu, G., Huang, J., & Lim, V. C. (2010). As (V) and As (III) Removal from Water by a Ce-Ti Oxide Adsorbent: Behavior and Mechanism. *Chemical Engineering Journal, 161,* 106-113. https://doi.org/10.1016/j.cej.2010.04.039

Liu, Y., Ohko, Y., Zhang, R., Yang, Y., & Zhang, Z. (2010). Degradation of Malachite Green on Pd/WO3 Photocatalysts under Simulated Solar Light. *Journal of Hazardous Materials, 184,* 386-391. https://doi.org/10.1016/j.jhazmat.2010.08.047

Mahlambi, M. M., Mishra, A. K., Mishra, S. B., Krause, R. W., Mamba, B. B., & Raichur, A. M. (2013). Metal Doped Nanosized Titania Used for the Photocatalytic Degradation of Rhodamine B Dye under Visible-Light. *Journal of Nanoscience Nanotechnology, 13,* 4934-4942. https://doi.org/10.1166/jnn.2013.7587

Mcyotto, F., Wei, Q., Macharia, D. K., Huang, M., Shen, C., & Chow, C. W. (2021). Effect of Dye Structure on Color Removal Efficiency by Coagulation. *Chemical Engineering Journal, 405,* Article ID: 126674. https://doi.org/10.1016/j.cej.2020.126674

Noor, T., Raffi, U., Iqbal, N., Yaqoob, L., & Zaman, N. (2019). Kinetic Evaluation and Comparative Study of Cationic and Anionic Dyes Adsorption on Zeolitic Imidazolate Frameworks Based Metal Organic Frameworks. *Materials Research Express, 6,* Article ID: 125088. https://doi.org/10.1088/2053-1591/ab5bdf

Shan, R. R., Yan, L. G., Yang, Y. M., Yang, K., Yu, S. J., Yu, H. Q. et al. (2015). Highly Efficient Removal of Three Red Dyes by Adsorption onto Mg-Al-Layered Double Hydroxide. *Journal of Industrial Engineering Chemistry, 21,* 561-568. https://doi.org/10.1016/j.jiec.2014.03.019

Shi, Y., Yang, Z., Xing, L., Zhou, J., Ren, J., Ming, L. et al. (2021). Ethanol as an Efficient Cosubstrate for the Biodegradation of Azo Dyes by *Providencia rettgeri*: Mechanistic Analysis Based on Kinetics, Pathways and Genomics. *Bioresource Technology, 319,* Article ID: 124117. https://doi.org/10.1016/j.biortech.2020.124117

Srinivasan, S., & Sadasivam, S. K. (2021). Biodegradation of Textile Azo Dyes by Textile Effluent Non-Adapted and Adapted *Aeromonas hydrophila*. *Environmental Research, 194,* Article ID: 110643. https://doi.org/10.1016/j.envres.2020.110643

Tehrani, M. S., & Zare-Dorabei, R. (2016). Highly Efficient Simultaneous Ultrasonic-Assisted Adsorption of Methylene Blue and Rhodamine B onto Metal Organic Framework MIL-68(Al): Central Composite Design Optimization. *RSC Advances, 6,* 27416-27425. https://doi.org/10.1039/C5RA28052D

Wei, F., Chen, D., Liang, Z., & Zhao, S. (2018). Comparison Study on the Adsorption Capacity of Rhodamine B, Congo Red, and Orange II on Fe-MOFs. *Nanomaterials, 8,* Article No. 248. https://doi.org/10.3390/nano8040248

Yang, Q., Lu, R., Ren, S., Chen, C., Chen, Z., & Yang, X. (2018). Three Dimensional Reduced Graphene Oxide/ZIF-67 Aerogel: Effective Removal Cationic and Anionic Dyes from Water. *Chemical Engineering Journal, 348,* 202-211. https://doi.org/10.1016/j.cej.2018.04.176

Zhang, K., Sun, D., Ma, C., Wang, G., Dong, X., & Zhang, X. (2020). Activation of Peroxymonosulfate by $CoFe_2O_4$ Loaded on Metal-Organic Framework for the Degradation of Organic Dye. *Chemosphere, 241,* Article ID: 125021. https://doi.org/10.1016/j.chemosphere.2019.125021

Zhang, Z., Yao, Z.-Z., Xiang, S., & Chen, B. (2014). Perspective of Microporous Metal-Organic Frameworks for CO_2 Capture and Separation. *Energy Environmental Science, 7,* 2868-2899. https://doi.org/10.1039/C4EE00143E

Zhao, S., Chen, D., Wei, F., Chen, N., Liang, Z., & Luo, Y. (2017). Removal of Congo Red Dye from Aqueous Solution with Nickel-Based Metal-Organic Framework/Graphene Oxide Composites Prepared by Ultrasonic Wave-Assisted Ball Milling. *Ultrasonics Sonochemistry, 39,* 845-852. https://doi.org/10.1016/j.ultsonch.2017.06.013